Nat. Hazards Earth Syst. Sci. Discuss., 3, 3621–3653, 2015
www.nat-hazards-earth-syst-sci-discuss.net/3/3621/2015/
doi:10.5194/nhessd-3-3621-2015
© Author(s) 2015. CC Attribution 3.0 License.

Natural Hazards and Earth System Sciences
Open Access
Discussions

This discussion paper is/has been under review for the journal Natural Hazards and Earth System Sciences (NHESS). Please refer to the corresponding final paper in NHESS if available.

Seeking for key meteorological parameters to better understand Hector

S. Gentile and R. Ferretti

Department of Physical and Chemical Sciences/CETEMPS, University of L'Aquila, Via Vetoio, 67010 Coppito, L'Aquila, Italy

Received: 30 April 2015 – Accepted: 11 May 2015 – Published: 4 June 2015

Correspondence to: S. Gentile (sabrina.gentile@aquila.infn.it)

Published by Copernicus Publications on behalf of the European Geosciences Union.

Abstract

Twelve Hector events, a storm developing in the northern Australia, are analyzed to the aim of identifying the main meteorological parameters involved in the convective development. Based on Crook's ideal study (Crook, 2001) wind speed and direction, wind shear, water vapor, Convective Available Potential Energy and type of convection are the parameters used for this analysis. Both European Centre for Medium-Range Weather Forecasts (ECMWF) analysis and high resolution simulations from the Fifth-Generation Mesoscale Model (MM5) are used. The MM5 simulations are used to connect the mean vertical velocity to the total condensate at the maximum stage and to study the dynamics of the storms. The ECMWF analysis are used to evaluate the initial conditions and the environmental fields contributing to Hector development. The analysis suggests that the strength of convection is largely contributing to the vertical distribution of hydrometeors. The role of total condensate and mean lifting vs. low level moisture, Convective Available Potential Energy, surface wind and direction is analyzed for shear and no-shear conditions to evaluate the differences between type A and B for real events. Results confirm the tendency suggested by Crook's analysis. On the other hand, Crook's hypothesis of low level moisture as the only parameter that differentiates between type A and B can be applied only if the events develop in the same meteorological conditions. Crook's tests also helped to asses how the the meteorological parameters contribute to Hector development in terms of percentage.

1 Introduction

Hector is a vigorous convective system that develops on the Tiwi Islands, two islands included in the "Maritime Continent" (Ramage, 1968), an area extending across the Indonesian archipelago, the north Australia and the New Guinea. This is one of the primary regions of global latent heat release contributing to the forcing of the planetary scale circulations (e.g. Hadley and Walker cells). The Tiwi Islands, located in the

NHESSD
3, 3621–3653, 2015

northern tropical part of Australia, produce regular tropical convection during the pre-monsoon and monsoon "breaks" seasons (from November to March) in response to the latent heat released during the diurnal cycle (Keenan and Carbone, 1992).

This storm has been analyzed during observing campaigns like ITEX (1988), MCTEX (1995), SCOUT-O3 (2005) and TWP-ICE (2006) whose aims were to better understand the triggering mechanisms and the meteorological parameters favorable to the convective development. Particularly MCTEX campaign collected many environmental factors that are known or believed to influence the initiation, organization, propagation and intensity of deep convection. In addition this dataset allowed to define two distinct forcing regimes leading to Hector (Carbone et al., 2000):

1. type A: resulting from the confluence and convergence of the sea breeze fronts;
2. type B: rising form the interaction among sea breeze and gust front convectively generated by cold pools.

Type A forcing may be viewed as nature's backup mechanism when the meteorological conditions don't allow the type B development.

Following these campaigns some ideal and real numerical studies have been performed to understand the forcing and the triggering mechanisms of this convective cell (e.g., Golding, 1993; Crook, 2001; Saito et al., 2001; Ferretti and Gentile, 2009; Gentile et al., 2014).

Golding (1993) used the U.K. Met Office's mesoscale model at 3 km resolution initialized by a sounding to examine two cases from ITEX. The results suggest that the model qualitatively reproduces the diurnal evolution of Hector, showing a clear relationship between the storm development and the island topography. Saito et al. (2001) used the Japanese Meteorological Institute's mesoscale model at 1 km resolution to simulate a case from MCTEX. The study highlights a good agreement between the simulations and observations and focuses on the five stages of the convective life cycle.

NHESSD
3, 3621–3653, 2015

Chemel et al. (2009) simulated the 30 November 2005 Hector event using two models the Advanced Research Weather Research Weather (ARW) and the Forecasting and the Met Office Unified Model with a resolution of 1 km. Both models reproduce the development of Hector fairly well even though the two simulated surface heat fluxes are very different. This would mean that the intensity of the storm is not be controlled only by this factor. The aim of the paper is to investigate the role of deep convection in the vertical transport of tropospheric air into the lower stratosphere. Chemel et al. (2009) conducted a further simulation with ARW in large eddy simulation (LES) mode, refining the grid spacing to 250 m, and concluded that the characteristics of the Hector storm are basically similar in time and space to those obtained in the 1 km resolution. Therefore a 1 km resolution is fine enough to simulate faithfully this storm.

In the study by Ferretti and Gentile (2009) two Hector events (one observed during SCOUT-O3 and one during TWP-ICE) have been investigated analyzing the dynamics and thermodynamics. Using MM5 mesoscale model at 1 km resolution over the Tiwi Islands several numerical experiments have been performed to the aim of understanding the forcing and triggering conditions for the Hector development. The study demonstrates the key role of the sea breeze, water vapor content and soil moisture content on the Hector growth. Moreover, Gentile et al. (2014) carried out a study for highlighting both the triggering factors and microphysical structure of a Hector event. The event was analyzed using MM5 model simulations, ground-based radar and TRMM satellite data to the aim of understanding the mechanisms leading to the convective development. The analysis of the horizontal and vertical structure at high temporal and spatial resolution produced by MM5 allows to establish the mechanisms for triggering Hector: sea breeze, gust front from previous convection and channeling effect by topography.

Zhu et al. (2013) simulated four cases of Hector storm by running the ARW model with a maximum horizontal resolution of 1 km incorporating and not incorporating the observations collected during the ACTIVE campaign. Only one (30 November 2005) of the four cases was well simulated by the run without the ingestion of observations. Three events (16 November 2006, 6 and 10 February 2006) can be simulated only if

NHESSD
3, 3621–3653, 2015

the model was run incorporating observations. The major deficiency deduced by (Zhu et al., 2013) in the simulations of Hector is the smaller size and the weaker intensity in comparison with the observations.

Simulations were performed for a Hector event observed on 30 November 2005 by Dauhut et al. (2014) using the Meso-NH model performed with a grid spacing of 1600, 800, 400, 200 and 100 m. The updraft generally decreases with reduced resolution due to the reduced entrainment into the base of the updrafts. Indeed, the strong updrafts in the boundary layer obtained by the three finest simulations reinforce the updrafts in the upper troposphere.

Crook (2001) performed an ideal study using both a linear and non linear flow models for assessing Hector convective system most important parameters. The low level moisture is found to be an important parameter for differentiating between type A and B. High values of low level moisture correspond to earlier convection, then the associated evaporational cooling produces cold pools that retard the further inland progress of the sea breezes. Hence, Hector type B develops because of the convergence of one of the sea breeze and the gust front related to previous convection. Hector type A, which is associated to low values of low level moisture, develops when the generation of precipitating cold pools is delayed so that the sea breeze fronts have time to converge. Moreover, Crook (2001) performed sensitivity tests to surface heating, wind speed and direction. The results show a strong link between convective available potential energy (CAPE), wind speed and direction and total condensate (sum of all hydrometeors) of Hector cells. The relationship between couple of meteorological parameters was investigated using diagrams that allowed to assess that the convective strength, in terms of vertical velocity, increases as the wind speed decreases and as the wind direction turns toward the major axis of the Tiwi Islands (Crook, 2001).

In this study, twelve Hector events (from November 1995 to November 2008) are used to investigate the portability to real events of the conclusions of Crook's study. To this aim the relationship between the same meteorological parameters, used by Crook, are investigated for the real Hectors, each one characterized by its own boundary and

NHESSD
3, 3621–3653, 2015

initial conditions. The case studies are simulated using the MM5 mesoscale model as described in Ferretti and Gentile (2009) and Gentile et al. (2014) and the results are investigated to establish the contribution of water vapor, surface wind speed and direction to the convective strength. These previous works (Ferretti and Gentile, 2009; Gentile et al., 2014) allow to assess the model ability in reproducing the dynamics and in correctly detecting the triggering factors leading to the Hector development by performing a detailed comparison with observations. However a temporal and spatial shift is found for MM5; that is a common issue found also for WRF by Chemel et al. (2009) and Zhu et al. (2013). The main focus of this study, as already pointed out, is to investigate the role of a few key meteorological parameters for Hector development by using the Crook's diagrams which are independent from time. Therefore, possible temporal or spatial shift in the MM5 simulations of Hector do not affect the results.

The study is organized as follow. A meteorological analysis of the events as a function of wind speed, wind direction and shear, CAPE and water vapor, convection modes A or B with a brief description of the model configuration is presented in Sect. 2. The comparison in terms of cloud total condensate and vertical velocity profiles among the twelve events is shown in the Sect. 3. The fourth paragraph describes the Crook's test and outlines the main features in terms of percentage involved in the Hector development. Conclusions are drawn in Sect. 5.

2 Meteorological characteristics of the Hector events

The convective strength of the tropical storm Hector is evaluated using the meteorological variables suggested by Crook (2001). In this study twelve real events (eight single cell and two double cell) are selected: some of them (20 and 23 November 1995; double cells 27 November 1995; 1 and 4 December 1995) were observed during the Maritime Continent Thunderstorm Experiment (MCTEX), a campaign held in late 1995 on the Tiwi Islands with the goal of monitoring the convective life cycle of the mesoscale convective system (Keenan and Carbone, 1992; Carbone et al., 2000).

NHESSD
3, 3621–3653, 2015

Four of the remaining events (the double cell 30 November 2005, 6 February 2006 and 29 November 2007) are already analyzed respectively by Ferretti and Gentile (2009) and Gentile et al. (2014). In what follows the events are named with the acronyms:

1. 20 November 1995: N20;
2. 23 November 1995: N23;
3. 27 November 1995: N27 (double cell);
4. 1 December 1995: D1;
5. 4 December 1995: D4;
6. 30 November 2005: N30 (double cell);
7. 6 February 2006: F6;
8. 29 November 2007: N29;
9. 11 November 2007: N11;
10. 17 November 2008: N17.

To simulate the events the same configuration as in Ferretti and Gentile (2009) and Gentile et al. (2014) is used. The mesoscale model MM5V3 is a non hydrostatic model at primitive equations fully compressible with a terrain following vertical coordinate (Dudhia et al., 2004). Four nested domains and 58 vertical levels are used: the mother domain has a 27 km grid, covering the tropical part of Australia. The finest domain has a horizontal grid of 1 km and it is centered over the Tiwi Islands. The following parameterizations are used: the Gayno-Seaman for the planetary boundary layer; the MM5 Cloud radiation scheme for radiative transfer processes; the Kain-Fritsch cumulus convection parametrization to domains 1, 2 whereas no cumulus convective parameterization for the finest domain; the Reisner 2 parametrization as microphysical scheme. To

NHESSD
3, 3621–3653, 2015

improve the meteorological analysis on the mesoscale grid, "direct" observations from surface and radiosonde have been incorporated using the objective analysis based on the Cressman scheme (Faccani et al., 2003). The simulations are initialized using ECMWF analysis at 0.25° and the boundary conditions are upgraded every 6 h and they last 24 h for all the events.

In the following subsections the ECMWF analysis are used to analyze the main dynamical aspects of the Hector events. The analysis is performed evaluating the role of the following parameters on the development of the Hector storm: the wind speed and direction at three different levels (lower (LL, 950 hPa), medium (ML, 700 hPa) and upper level (UL, 300 hPa)), the CAPE and the water vapor content (mixing ratio). The values of these parameters for the Hector events are summarized in Table 1. To better understand the dynamical conditions for the storm development, two parameters are added: the shear occurrence and the typology of the events (definition based on Carbone et al., 2000). All these quantities are derived from the ECMWF analysis at the 00:00 UTC (09:30 LST); for the second cells (tagged in the Table as 2) the meteorological parameters are extracted six hours later that is at the 06:00 UTC (15:30 LST).

2.1 Wind Speed

The wind speed at the surface controls the magnitude of convective instability over the Tiwi Islands; indeed, as the wind speed decreases, the low level air mass spends more time over the heated and moistened island increasing its instability (Crook, 2001).

The Hector D1 and N29 present weak wind at the surface with a maximum of $2.5\,m\,s^{-1}$ (Table 1) from south for D1 and from east for N29 (Fig. 1a–e). Also N17 and N20 are characterized by very weak wind at the lower level with a maximum speed of $2\,m\,s^{-1}$, respectively from south-east and north but in addition weak wind is also found at 700 hPa (Fig. 2c–f). These conditions are favorable for increasing the instability which allows for the vertical growth of the tropical thunderstorm. On the contrary, N11 and F6 show at the middle level respectively a very strong south-easterly wind up to 16–18 $m\,s^{-1}$ and a moderate easterly wind of $8\,m\,s^{-1}$ (Figs. 2b and 3b) allowing to

NHESSD
3, 3621–3653, 2015

suppose more stable conditions and unfavorable environment for the vertical growth. D4 and N23 have very similar wind structure, both events have a weak westerly flow (less than $3\,m\,s^{-1}$) at the lower levels (Figs. 1c and 3c) and a sharp change of wind direction at the middle level with a speed of approximately $5\,m\,s^{-1}$ (Figs. 1d and 3d). Finally, the initial conditions of N27 (double cell event) show a very weak surface wind characterized by a speed of 1.5–2.5 $m\,s^{-1}$ (Fig. 4e and Table 1) produced by an area of high pressure centered on the Tiwi Islands (Fig. 4f). On the contrary, the double cell event (N30) shows a moderate wind speed (approximately $5\,m\,s^{-1}$) at the three levels changing direction at higher altitude (Table 1, Fig. 4a and b). For these two events the environmental conditions prior the organization and the development of the second convective cell are more unstable and disorganized than the single cell events, as suggested by the fast low level wind (Table 1, Fig. 4c, g, d and h) produced by the gust front of the previous cell.

2.2 Wind direction and shear

The wind direction is another meteorological parameter affecting the Hector development. Assuming that the Tiwi Islands have an ellipse shape, if the air mass blows along the major axis (east-west), the low level convergence, produced by the sea breeze and the surface wind, is maximized because of the longer time spent by the air mass over the heated and moistened surface of Tiwi Islands. On the contrary, if the air mass is blowing along the minor axis (north-south), the low level convergence is reduced both by the shorter time spent by the air mass over the heated surface and by the overlapping of the surface wind in the same direction of the sea breeze, producing a much weaker convection (Crook, 2001). In addition, the vertical wind shear (change of direction) enhances the instability allowing for the vertical growth of the cell (Crook, 2001).

The D4, F6 and N23 events show a similar flow structure characterized by a strong and sharp vertical wind shear (Table 1); the westerly surface wind (Figs. 1c and 3a and c) turns of 180° becoming easterly at middle level (Figs. 1d and 3b and d). The Hectors N11 and N20 show shears from a different direction: a surface flow from south-west

NHESSD
3, 3621–3653, 2015

and from north (Fig. 2a–e respectively for N11 and N20) and a strong south-easterly (N11, Fig. 2b) and moderate south wind (N20, Fig. 2f) at the middle level respectively. Figures 1a–e and 2c show the lack of a change in the wind direction between the low and the middle level which confirms the absence of the shear (Figs. 1b–f and 2d) for D1, N29 and N17. Finally, the two double cell events: no wind shear is detected for N27 (Fig. 4e and f), the easterly wind is constant up to middle level; a strong vertical wind shear is found for N30 (Fig. 4a and b), the lower level wind turns from a north-westerly to a easterly at 700 hPa. This structure lasted till the onset of the second cell (Fig. 4c and d). For what concern the environment in which the second convective cell develops, it is more heterogeneous: the onset of a weak wind shear helps to develop the N27 second cell (Table 1, Fig. 4g and h); a strong vertical wind shear is still on for N30 second cell (Table 1, Fig. 4c and d).

2.3 CAPE and water vapor

The CAPE is derived from the vertically integrated buoyancy of an air parcel and it is an indicator of atmospheric instability. Results from the MCTEX campaign showed that the variability of CAPE is mainly due to the variability of the low level moisture. Therefore, the two parameters are directly proportional (Crook, 2001).

Four single cell cases are characterized by high values of CAPE (greater than 1200 $J\,kg^{-1}$ and lower than 2500 $J\,kg^{-1}$): D1, D4, N23 and N29 (Table 1). All these events show a remarkable convective activity with several cells developing before and/or after the main Hector cell. The double cell events present: wet conditions with high value of CAPE (2000 $J\,kg^{-1}$) and relative humidity (18–19 $g\,kg^{-1}$, Table 1) for N30; dry environment with low CAPE (450 $J\,kg^{-1}$) and water vapor mixing ratio (16–18 $g\,kg^{-1}$, Table 1) for N27. However, the second convective cell develops in a more unstable environment for both events: CAPE remains close to 2000 $J\,kg^{-1}$ for N30 and increased up to 1650 $J\,kg^{-1}$ for N27 (Table 1).

The following events were characterized by low values (between 150 and 650 $J\,kg^{-1}$) of CAPE (Table 1): N11, N17, N20 and F6, inferring a weak convective activity.

NHESSD
3, 3621–3653, 2015

2.4 Convection type A or B

Convection of type A or B is a simple way to differentiate the dynamical development of the storm; type A convection is generated by the convergence of two sea breeze fronts (Carbone et al., 2000); whereas type B is generated by the convergence of a single sea breeze front and a cold pool produced by previous convection (Crook, 2001; Gentile et al., 2014).

For both double cell events (N27 and N30), the first convective cell develops from the convergence of the two sea breeze fronts (type A) and the second one from the interaction of the gust front of the first decaying cell (type B) with the north and the south sea breeze front, respectively for N27 and for N30 (an exhaustive description of the meteorological characteristics of N30 is given by Ferretti and Gentile, 2009). The dynamics of the storm is very similar for both the events: the first precipitating cells develop in north-eastern part of Melville Island at approximately 12:00 LST. In the following hours, the convective system reaches a first maximum of reflectivity of 55–60 dBz associated to a strong convective cell (Fig. 5b and Fig. 14b of Ferretti and Gentile, 2009), that reaches a height of 16 km at 13:10 LST for N27 (Fig. 5a) and 14 km at 14:30 LST for N30 (Fig. 14b of Ferretti and Gentile, 2009). The maximum development of the second cells is reached at 16:10 LST with a height of 16–17 km for N27 (Fig. 5c and d) and at 15:50 LST with a height of 16 km for N30 (Fig. 14c and d of Ferretti and Gentile, 2009).

For D1 the maximum development of the storm is reached at 15:10 LST with a height of 16 km (Fig. 5e and f) after the organization and aggregation of several convective cells. The precipitation starts at the 13:00 LST in the northern part of the islands and a first deep cell develops at 13:50 LST, this last one contributes to the Hector growth (type B).

Two different Hector development are found for D4 and N23, although the rain starts with the front of the south sea breeze for both events (at 13:00 LST for the first and 10:30 LST for the second event). This leads to a first convective tower reaching 10–11 km at the 13:10 LST that finally brings to the maximum development (type B) at

NHESSD
3, 3621–3653, 2015

16:50 LST with a height of 17 km for D4 (Fig. 5g and h), whereas for N23 the convective line moves quickly to the north west of the Tiwi Islands and interacts with the north breeze front triggering the development of the Hector cell (maximum of 15 km at 12:50 LST, Fig. 6a and b). This is why N23 can be classified as type A (Table 1).

Also N29 (a detailed description of this event can be found in Gentile et al., 2014) is Type B; the development of this convective event is characterized by non precipitating and well organized cells during the first stage that ends as weak precipitation starts. Hence, the cells merge into a convergence line, that interacting with the south sea-breeze front, strengthened by a channeling effect, produces an intense growth of the convection. This phase corresponds to the mature stage characterized by a cloud top height reaching 18 km (Fig. 13a and b of Gentile et al., 2014).

The N11 dynamical evolution is characterized by an intense convective activity leading to type B development: a first cell appears in the northern part of the islands at 15:50 LST that triggers the vigorous Hector cell. A maximum height of 19–20 km is reached at the 17:10 LST in the middle area of the Tiwi's (Fig. 6c and d). Similarly for N17 (type B): the gust front, related to a first precipitating cell developed at 15:50 LST in the eastern part of the Tiwi Islands, interacts with the south sea breeze front leading at 16:30 LST to a maximum height of 16–17 km (Fig. 6e and f). Also N20 is classified as type B (Table 1): its first stage is characterized by aligned non precipitating convective cells. These cells lead to an initial double structure that merges in a unique Hector cell at 17:10 LST; the maximum development shows a height of 17 km (Fig. 6g and h). Finally F6 (a detailed description of the meteorological characteristics is given in Ferretti and Gentile, 2009) is characterized by two precipitating cells: the first one developing at 12:30 LST in the eastern part of Tiwi Islands, then decaying at 14:30 LST in the central area; the second deep cell reaches the maximum reflectivity of 45–50 dBz at 15:30 LST with a maximum cloud top of 16 km (Fig. 14e and f of Ferretti and Gentile, 2009). The interaction between the gust front of the decaying first cell with the south breeze front is the triggering mechanism for this Hector event (type B).

NHESSD
3, 3621–3653, 2015

3 Cloud total condensate and vertical velocity profiles for the events

In order to better understand the mechanisms leading to different convective structure for these Hector events, the vertical structures of the storms is analyzed in terms of total condensate (Crook, 2001). To this aim MM5 simulations are used to extract the mean vertical profile of the cloud total condensate (sum of all hydrometeors) and the vertical velocity for each event at the maximum stage (Fig. 7). The maximum stage is selected based on the time of the storm maximum height. The profiles are spatially averaged for each layer within the volume encapsulating Hector at a specific time. The maximum of the mean vertical velocity profile is approximately $0.9\,m\,s^{-1}$ for N11 (Fig. 7d) and the largest vertical velocity is $35\,m\,s^{-1}$ for the same event. Also D1, D4, N29, N17 and the first and the second cell, respectively, for N27 and N30, have a maximum updraft value exceeding $20\,m\,s^{-1}$; if spatially averaged it does not exceed $0.6\,m\,s^{-1}$. The values of the maximum vertical velocity for N30 are very close to those obtained with the LES simulations by Dauhut et al. (2014); the maximum updraft obtained by MM5 is approximately $22\,m\,s^{-1}$ sustained for a height up to 8 until 16 km (not shown), structure very close to the one simulated by Meso-NH using a horizontal resolutions of 400, 200 and 100 m (Fig. 3a in Dauhut et al., 2014).

The absolute maximum of the total condensate matter is approximately $1.5\,g\,m^{-3}$ for the first cell of N27 (Fig. 7e), but the largest vertical velocity is not reached by this event.

The vertical velocity profiles (Fig. 7b, d and f) present common features for most of the events: at the lower level a weak downdraft related to the precipitating hydrometeors prevails, and at the upper level, a very strong updraft can be detected associated to the latent heat release due to the condensation process. In addition, a downdraft peak in the vertical velocity profile is found at the same level of a relative maximum in the total condensate profile for: N11 at 2 km (Fig. 7c and d); the second cell of N30 at 3 km (Fig. 7e and f); the first cell of N27 at 3–4 km (Fig. 7e and f). These would suggest that the downdraft is related to the sinking due to the melting or evaporation cooling, and the

NHESSD
3, 3621–3653, 2015

corresponding total condensate maximum to the production of rain or melted graupel. Moreover, the total condensate maxima are at higher altitude than the updraft peaks as for N29, N20 and N11 (Fig. 7b and d): these events have the maximum updraft at approximately 12 km and show a relatively large amount of total condensate up to 14–16 km (Fig. 7a–c). On the other hand, if the maximum vertical velocity is positioned at lower levels, the most part of the hydrometeors distribution is at lower level too. A clear example is the first cell of the N27 (Fig. 7e and f): the maximum updraft is located at approximately 4 km and the largest part of hydrometeors is below 10–12 km.

The maximum total condensate and its vertical distribution, may be related to the strength of convection which is generally stronger if generated by the convergence of downdraft of previous cells and the sea breeze front (type B) than the one generated by the convergence of the two sea breeze fronts (type A) (Crook, 2001). Therefore, larger vertical velocities are expected for type B events; indeed, the largest vertical velocity is found for N11, which is Type B. The previous analysis suggests that the strength of convection is largely contributing to the vertical distribution of the total condensate. Therefore, the structure of these Hector events agree with the Crook (2001) hypothesis and allows for establishing that the strength of the event is proportional to the total condensate. However, the large variability of the total condensate vertical distribution among type A's and B's suggests that other parameters are playing an important role beside the strength of convection.

4 Crook's test to detect triggering factors

In this section the analysis of the real events is carried out using the Crook's diagrams as "benchmark".

Based on ideal studies of Hector, Crook (2001) suggested that the amount of total condensate is strongly related to the low level moisture, in term of CAPE, as well as to the surface wind velocity and direction. Therefore, a model aided analysis of the total condensate and of a few meteorological parameters (wind speed and direction,

NHESSD
3, 3621–3653, 2015

and CAPE), as used by Crook (2001), may help to highlight the most important factors for the previously Hector events. To this aim the same analysis performed by Crook (2001) is applied to the real Hector events analyzed in this study but some differences are obviously present. The possibility of changing the meteorological parameters as for example keeping constant one field as is done by Crook (2001) is not applied because it has already been verified its disruptive effect on Hector. Indeed, for real events the variation of a parameter cause the lack of the Hector development, for example in the work of Ferretti and Gentile (2009) the halving and the increasing of the initial water vapor content disabled the Hector development.

The following MM5 meteorological parameters are used for the analysis: low level moisture, in term of CAPE, surface wind speed and direction. Following Crook (2001), the variables are analyzed at the *model start time*, that is several hours before the Hector development. For the single events and for the first cell of double events the analysis is performed at 08:30 LST; whereas for the second cell of double events, the ending time of the first cell is taken as reference: 15:10 LST for N30 and 15:30 LST for N27.

All the meteorological parameters are analyzed vs. total condensate and mean lifting (vertical velocity at 500 m) as in Crook (2001). The vertical velocity is extracted three hours before the maximum development of Hector and is averaged all over the island surface; the total condensate, instead, is averaged within the volume encapsulating Hector at the maximum stage. Also CAPE, surface wind speed and direction are averaged all over the surface of the Tiwi Islands. To the aim of understanding the convective response to the flow direction either along the major (90°) or minor axes (0°) of the islands, the wind direction is projected in the first quarter of the wind rose.

Crook (2001) analyzed the vertical velocity wind respect to the surface wind velocity and direction (Fig. 7b and c in Crook, 2001) related to shear and no-shear conditions. Hence, Fig. 8 shows the results by Crook and the Hector events, respectively gray lines and twelve symbols representing the Hector events. A few events closely follow the shear (F6, N20 and the second cell of N27 and N30) and no-shear (D1 and N29) lines

NHESSD
3, 3621–3653, 2015

(Fig. 8a) or they belong to the right zone (i.e. no shear zone for the first cell of N27), confirming for the shear events the correlation between the decrease of the vertical velocity and the surface wind increase. A few cases do no show any specific signal, probably because the real atmosphere is more complex than the ideal one and more than one parameter is contributing to the vertical lifting as for example the topography or the convergence line. Therefore, the ideal response can be used to sort the events: more the position of the event in the diagram is close to the "ideal" one and more the meteorological parameter contribute to the convective strength.

The second cells of both the double structure events show a stronger surface wind speed than the corresponding first cell; this is due to the gust front associated to the downdraft of the previous convective cell. This is why the double cell events are not aligned with the others.

A similar analysis is performed for the vertical velocity as function of the surface wind direction. The results clearly show (Fig. 8b) that most of the events are located in the right position except for four events: D1, N17, N29 and N23, suggesting difficulties in the real atmosphere to completely separate the two regimes. However, it confirms roughly the increase of the vertical velocity when the flow is eastward (90°). This supports the hypothesis of greatest lifting when the flow is along the major axis of the island as assessed by Carbone et al. (2000) and Crook (2001). It is useful to highlight that the wind direction related to the second cells of the double events does not show a clear signal because at this time the sea breeze regime is either well developed or destroyed, and "leftover" from the first cell is affecting the environment. Therefore, their positions in the graph have an uncertainty larger than one for the single cell events.

The analysis of the total condensate vs. wind speed (Fig. 9a) shows that most of the Hector events are aligned along a line having a slope close to that of Crook one but a smaller intercept (gray dotted line in Fig. 9a) suggesting a sort of "bias" between the Crook's ideal and the real atmosphere. This disagreement can be explained by speculating that the "real" events need weaker surface wind than the "ideal" one to produce the same total condensate. Based on this hypothesis a new reference line can be as-

NHESSD
3, 3621–3653, 2015

sumed, then only two events are out of the distribution: the second events of the double Hector N27 and N30 (Fig. 9a, white square and white star respectively). Both events have larger wind speed than the expected one on equal terms of normalized total condensate. The absolute maximum of total condensate is reached by the first cell of N27, whereas the second cell shows approximately a 65 % of the first cell total condensate. On the contrary, for N30 the second cell is stronger than the first one, in terms of cloud total condensate. This is partly due to the leftover of the previous cell because of the very short time interval (1 h and 20 min) occurred between the two maxima. Whereas for N27 the second cell develops 3 h later than the first one making the two cells more independent than the previous event. Hence, the hypothesis of increasing of the total condensate as the surface wind speed decreases (Fig. 9a) is still confirmed, but below $4\,m\,s^{-1}$ for all single cell events and for the first cell of double ones. Based on the results of the dry linear and non-linear models, Crook (2001) assessed that the relationship between convective strength and low level convergence (i.e. surface wind speed) is not strictly monotonic because the convective strength did not continue to increase as the flow decrease below $4\,m\,s^{-1}$. The twelve Hector events reproduce a monotonic relationship also below $4\,m\,s^{-1}$ (Fig. 9a). This discrepancy between the simulations of the real events and the Crook experiments is not surprising and it may be due to the differences between the models assumptions and the use of an idealized sounding in the Crook study.

All Hector events, except the second cell of N27 and N17, confirm the increase of the total condensate if the low level flow is along the major axes as showed by the plot of the total condensate vs. the wind direction (Fig. 9b), but a spread along the Crook "theoretical" line is found for the real events. As for the mean lifting vs. wind direction (Fig. 8b) the major difference between the Crook ideal behavior and real one is found for the surface wind whose direction is close to the minor axes. But the Crook's hypothesis of maximizing the low level convergence if the flow is aligned along the major axis of the Tiwi Islands is confirmed.

NHESSD
3, 3621–3653, 2015

Finally, similarly to what was done by Crook (2001), the total condensate vs. the low level moisture, express in term of CAPE is analyzed. The Hector events do not show a clear signal, but a slight increase of the total condensate as the CAPE increase is found, except for the first cell of N27. This is completely out of the Crook's line (Fig. 9c gray square). Moreover, on the contrary to what found by Crook (Fig. 13a in Crook, 2001), no maximum is found for the total condensate vs. CAPE because of the lack of Hector's values around the theoretical maximum; hence it is not possible to assess its occurrence.

4.1 Main features of the Hector events

Based on the previous analysis and on the brief summary of the main characteristics of these Hector events given in Table 1 some important highlights can be inferred using the surface wind speed, surface wind direction and CAPE. Each event seems to be driven by particular meteorological conditions, whose contributions to the convective strength have been estimated and summarized in the Table 2. This computation is performed by evaluating the distance between the "real" point and its corresponding "ideal" one. Once obtained the percentages from surface wind speed, surface wind direction and CAPE, the total contribution from the three parameters is normalized to 100. Therefore, the percentage of influence for each parameter is calculated and the following conclusions can be drawn:

1. D1 and N29 events, both type B, produce large amount of total condensate (respectively 75 and 82 % of the maximum) suggesting a strong convective strength. A similar contribution (≈ 33 %) to the Hector development is found for the three meteorological parameters, with a prevalence of favorable surface flow direction for the first event and slow surface wind velocity for the second one (Table 2).

2. D4, F6, N17, N23 and the first cell of N27 have a total condensate ranging between 55 and 65 % of the maximum (except for the first cell of N27 that is the maximum). The convective development is due mainly (percentage of its influence

NHESSD
3, 3621–3653, 2015

from 47 to 62 %) to just one meteorological parameter: surface flow direction for D4, F6 and N24; slow wind speed for N17 and N27. Another important contribution for three of these events is also found: the surface wind speed for F6, the low level moisture for N23 and the wind direction for the first cell of N27.

3. The development of N11 and both cells of N30 is sustained by the "right" CAPE value (Crook, 2001) and by the wind direction. Indeed, the flow is blowing along the major axis of the Tiwi Islands maximizing the low level convergence. The N30 (type B) produces a larger amount of total condensate (58 % for the second cell vs. 35 % of the first one) than the type A suggesting a stronger convective strength; the most important parameter to justify it is the low level wind shear. Indeed, the Crook's analysis allows for highlighting the change in the regime from no-weak shear for the first cell to strong shear for this second cell, whereas the other meteorological parameters are similar for both. The N30 (type A) produces the smallest amount of total condensate suggesting a weak convective strength; several meteorological parameters justify it. The large surface velocity, the wind direction and a weak shear are not sustaining Hector, whereas CAPE is the only acting positively.

4. N20 and the second cell of N27 are characterized by a total condensate around 50–60 % of the maximum content but the events present a strong mean lifting. The convective strength for both events mostly depends on two parameters with different weights: the main contribution (approximately 42 %, see Table 2) is coming from the slow wind speed for N27 and CAPE for N20. Moreover, slow wind speed and CAPE contribute for 35 % respectively to N20 and N27 development.

In summary, the previous analysis highlights the role of the meteorological parameters in defining the Hector convective strength, but it does not allow to highlight a specific parameter as Crook assessed for the low level moisture to establish the Hector typology. Moreover, the relationship between both the total condensate and mean lifting and

NHESSD
3, 3621–3653, 2015

several meteorological parameters for the Hector events is confirming what found by Crook (2001) within this sensitivity analysis.

5 Conclusions

In this study twelve Hector events are analyzed using MM5 model simulations to the aim of highlighting the main meteorological parameters and their role in triggering convection. A brief meteorological analysis of the events is performed using CAPE, water vapor, wind speed and direction and typology of convection. Moreover, a comparison in terms of mean total condensate vertical profiles and mean vertical velocity at the maximum development is carried out. The applicability of the Crook's hypothesis to real cases is explored verifying the linear relationship between both the convective strength and the total condensate vs. the low level moisture, expressed in terms of CAPE, surface wind speed and direction. The Crook's tests allow for concluding the following:

1. The strength of convection, in terms of mean lifting and total condensate, increases if the wind direction tends to be parallel to the major axes of the Tiwi Islands and if the wind speed surface decreases.

2. It is not confirmed the Crook's assumption on the low level moisture as the parameter differentiating between the type A and B modes of convection.

3. The previous hypothesis is verified for the two N30 Hector cells, where the second cell (type B) has a low level moisture and a convective strength larger than the first cell (type A). This would suggest the applicability of a type A or B classification based on the low level moisture for the events developing in the same meteorological conditions only. That means it cannot be generalized to all real cases.

NHESSD
3, 3621–3653, 2015

4. The meteorological parameters contributing to the Hector development are: only one by 47 % for five events; two by 32 % and less than 27 % for five events; all the paramereters by 31 to 37 % for only two cases.

Thanks to their simple orography and shape Tiwi Islands can be used as a laboratory to study the triggering factors contributing to convection. Hence, in this context this study will allow for better understanding different meteorological parameters concurring to the onset of convection even in complex orography regions.

Acknowledgements. NCAR is acknowledged for MM5 model. ECMWF is acknowledged for data analysis.

References

Carbone, R., Wilson, J., Keenan, T., and Hacker, J.: Tropical island convection in the absence of significant topography. Part I: Life cycle of diurnally forced convection., Mon. Weather Rev., 128, 3459–3480, 2000. 3623, 3626, 3628, 3631, 3636

Chemel, C., Russo, M., Pyle, J., Sokhi, R., and Schiller, C.: Quantifying the Imprint of a Severe Hector Thunderstorm during ACTIVE/SCOUT-O3 onto the Water Content in the Upper Troposphere/lower Stratospere, Mon. Weather Rev., 137, 2493–2514, doi:10.1175/2008MWR2666.1, 2009. 3624, 3626

Crook, N.: Understanding Hector: the dynamics of Island thunderstorm, Mon. Weather Rev., 129, 1550–1563, 2001. 3622, 3623, 3625, 3626, 3628, 3629, 3630, 3631, 3633, 3634, 3635, 3636, 3637, 3638, 3639, 3640

Dauhut, T., Chaboureau, J., Escobar, J., and Mascart, P.: Large-eddy simulations of Hector the convector making the stratosphere wetter., Atmos. Sci. Lett., 16, 135–140, doi:10.1002/asl2.534, 2014. 3625, 3633

Dudhia, J., Dave, G., Manning, K., Wang, W., and Bruyere, C.: MM5 Modeling System Version 3., PSU/NCAR Mesoscale Modelling System Tutorial Class Notes and User's Guide, Mesoscale and Microscale Meteorology Division of National Center for Atmospheric Research, 2004. 3627

NHESSD

3, 3621–3653, 2015

Faccani, C., Ferretti, R., and Visconti, G.: High-resolution weather forecasting over complex orography: sensitivity to the assimilation of conventional data, Mon. Weather Rev., 131, 136–154, 2003. 3628

Ferretti, R. and Gentile, S.: A study of the triggering mechanisms for deep convection in the Tropics using a Mesoscale Model: Hector events during SCOUT-O3 and TWP-ICE campaigns, Atmos. Res., 93, 247–269, 2009. 3623, 3624, 3626, 3627, 3631, 3632, 3635

Gentile, S., Ferretti, R., and Marzano, F.: Investigating Hector convective development and microphysical structure by high resolution model simulations, ground-based radar data and TRMM satellite data, J. Atmos. Sci., 71, 1353–1370, 2014. 3623, 3624, 3626, 3627, 3631, 3632

Golding, B.: A numerical investigation of tropical island thunderstorms, Mon. Weather Rev., 121, 1417–1433, 1993. 3623

Keenan, T. and Carbone, R.: A preliminary morphology of precipitation system in tropical northern Australia, Q. J. Roy. Meteor. Soc., 118, 283–326, 1992. 3623, 3626

Ramage, C.: Role of a tropical "Maritime Continent" in the atmospheric circulation, Mon. Weather Rev., 96, 365–370, 1968. 3622

Saito, K., Keenan, T., Holland, G., and Puri, K.: Numerical simulation of the diurnal evolution of tropical island convection over the maritime continent, Mon. Weather Rev., 129, 378–400, 2001. 3623

Zhu, M., Connolly, P., Vaughan, G., Choularton, T., and May, P.: Numerical simulation of tropical island thunderstorms (Hectors) during the ACTIVE campaign, Meteorol. Appl., 20, 357–370, doi:10.1002/met.1295, 2013. 3624, 3625, 3626

NHESSD

3, 3621–3653, 2015

Table 1. Meteorological characteristics of the Hector events extracted from ECMWF analysis at 00:00 UTC (09:30 LST) for all the single and first cell of the double structure events (tagged in the Table as 1) and at 06:00 UTC (15:30 LST) for the second cell (tagged in the Table as 2). In the heading LL stays for low level (950 hPa), ML for medium level (700 hPa), UL for upper level (300 hPa); wind shear is "yes" if there is a change of wind direction between LL and ML.

Events	Wind speed/dir LL ($m\,s^{-1}$ – deg)	Wind speed/dir ML ($m\,s^{-1}$ – deg)	Wind speed/dir UL ($m\,s^{-1}$ – deg)	Shear	CAPE ($J\,kg^{-1}$)	q ($g\,kg^{-1}$)	Type
D1	1.5–2.5 – S	8–7 – SE	0.5–1.5 – E	yes	1350	17–20	B
D4	2–2.5 – W	5.5–6 – E	6.5–7.5 – W	yes	1170	18–19.5	B
F6	2.5–3.5 – SW	7–8 – E	5–5.5 – E	yes	175	16.5–17.5	B
N11	3–4 – SSW	16–18 – SE	7–9 – NW	yes	650	17.5–21	B
N17	1–2 – SE	1.5–2 – E	8–9 – W	no	450	16–18	B
N20	< 1 – N	3–4.5 – S	12–16 – WSW	yes	650	16.5–17.5	B
N23	2.5–3.5 – W	4–5 – ESE	10–12 – NW	yes	2500	18.5–19.5	A
N27-1	1.5–2.5 – ENE	6–7 – E	2.5–4 – W	no	450	16–18	A
N27-2	2.5–3.5 – NNE	4.5–5.5 – ENE	3–5 – W	yes	1650	18–20	B
N29	1–2.5 – E	15–16 – ESE	7–8.5 NE	no	2000	18–19.5	A
N30-1	3.5–4 – NW	4–5 – ESE	3–5 – SW	yes	2000	18–19	A
N30-2	3–5 – W	3–4 – ENE	2–5 – SW	yes	1800	16–18.5	B

NHESSD
3, 3621–3653, 2015

Table 2. Percentage of influence for the meteorological parameters on the convective development of the Hector events.

Events	Surface wind speed	Surface wind direction	CAPE
D1	33 %	35 %	32 %
D4	26 %	47.5 %	26.5 %
F6	39 %	57 %	4 %
N11	27 %	34 %	39 %
N17	62 %	18 %	20 %
N20	32 %	25.5 %	42.5 %
N23	13 %	50 %	37 %
N27-1	47 %	38.5 %	14.5 %
N27-2	42 %	20 %	38 %
N29	37 %	31 %	32 %
N30-1	17.5 %	36.5 %	46 %
N30-2	22 %	38 %	40 %

NHESSD
3, 3621–3653, 2015

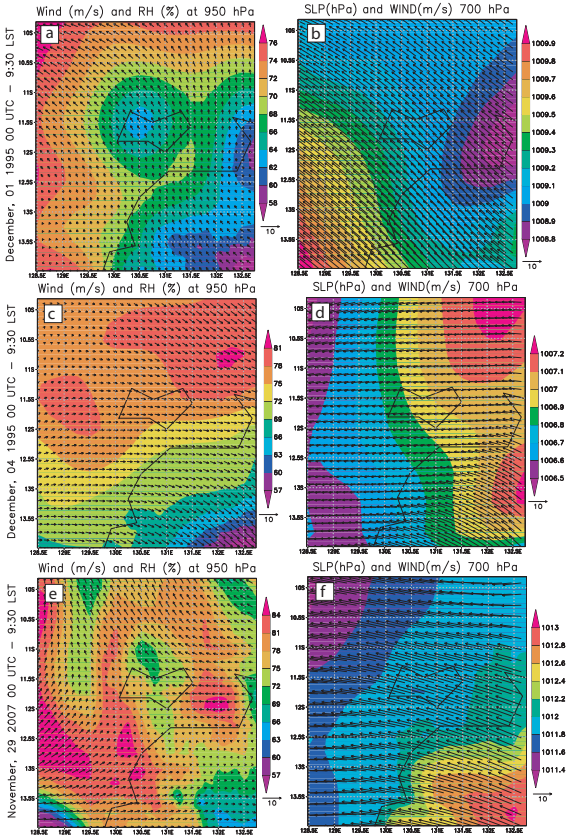

Figure 1. ECMWF analysis over the Tiwi Islands at 00:00 UTC for D1, D4 and N29. **(a)**, **(c)** and **(e)** reports surface wind and relative humidity at 950 hPa; **(b)**, **(d)** and **(f)** sea level pressure in filled contours and wind flow vectors at 700 hPa.

NHESSD
3, 3621–3653, 2015

Seeking for key meteorological parameters to better understand Hector

S. Gentile and R. Ferretti

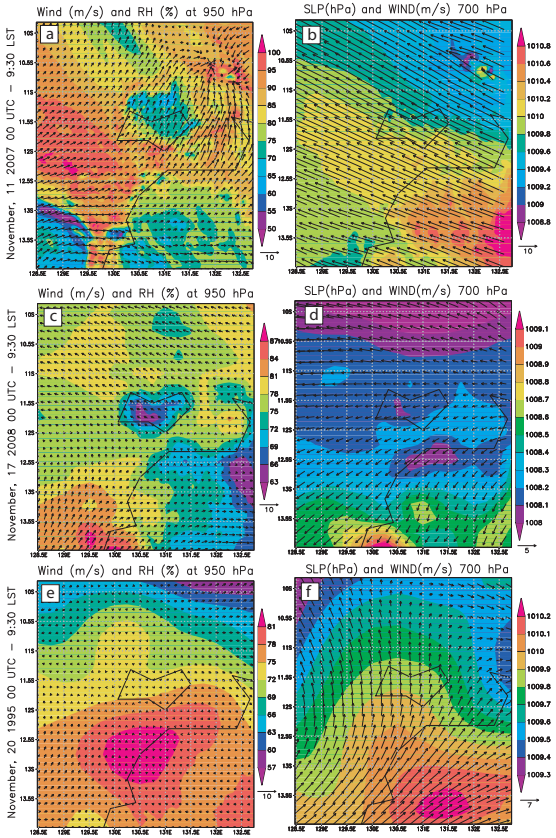

Figure 2. ECMWF analysis over the Tiwi Islands at 00:00 UTC for N11, N17 and N20. **(a)**, **(c)** and **(e)** reports surface wind and relative humidity at 950 hPa; **(b)**, **(d)** and **(f)** sea level pressure in filled contours and wind flow vectors at 700 hPa.

NHESSD
3, 3621–3653, 2015

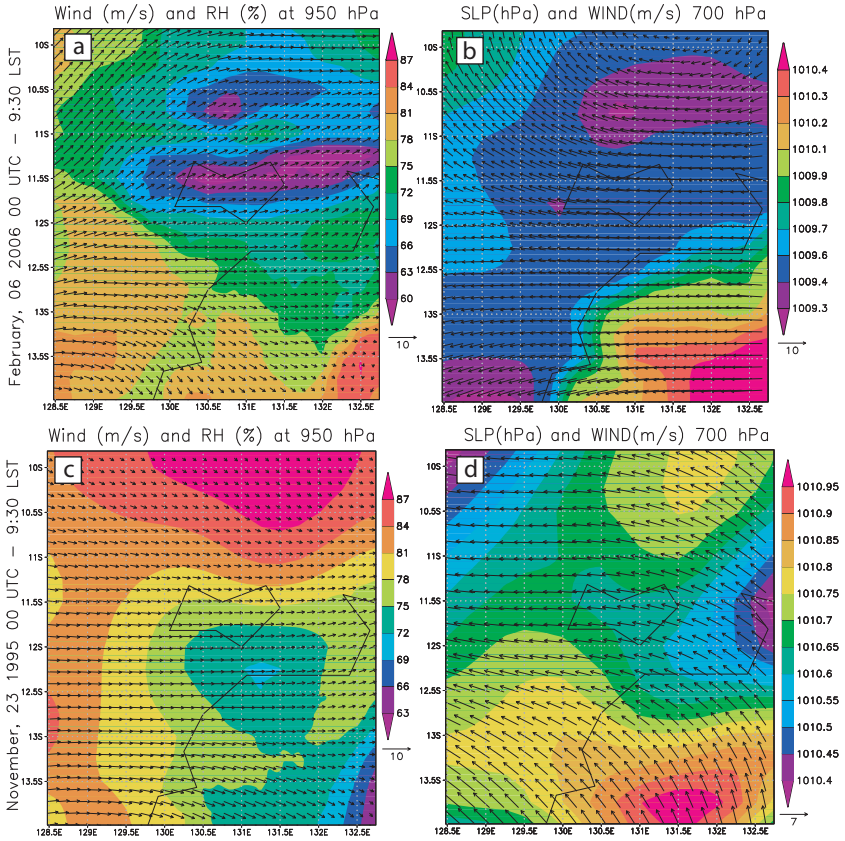

Figure 3. ECMWF analysis over the Tiwi Islands at 00:00 UTC for F6 and N23. **(a)** and **(c)** reports surface wind and relative humidity at 950 hPa; **(b)** and **(d)** sea level pressure in filled contours and wind flow vectors at 700 hPa.

NHESSD
3, 3621–3653, 2015

Seeking for key meteorological parameters to better understand Hector

S. Gentile and R. Ferretti

CC BY

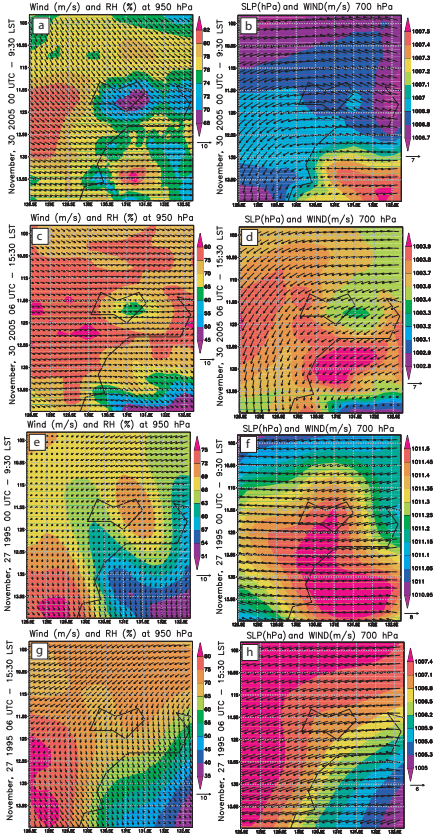

Figure 4. ECMWF analysis over the Tiwi Islands for N30 and N27 at 00:00 UTC for the first cell and at 06:00 UTC for the second one. **(a)**, **(c)**, **(e)** and **(g)** reports surface wind and relative humidity at 950 hPa; **(b)**, **(d)**, **(f)** and **(h)** sea level pressure in filled contours and wind flow vectors at 700 hPa.

NHESSD
3, 3621–3653, 2015

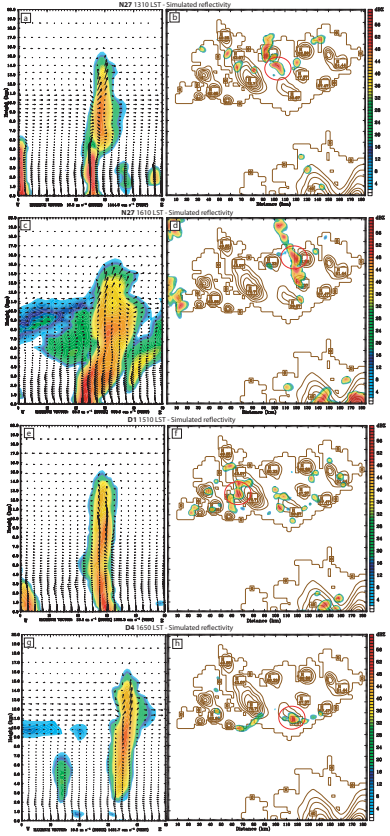

Figure 5. Sections at the maximum development of the Hector events N27 (double cell), D1 and D4. **(a)**, **(c)** and **(e)** Simulated vertical radar reflectivity (dBZ; filled color) and vertical wind, the section is taken along the red circle reported in the right panel. **(b)**, **(d)** and **(f)** Horizontal radar reflectivity (dBZ; filled color) and topography (brown).

NHESSD
3, 3621–3653, 2015

Seeking for key meteorological parameters to better understand Hector

S. Gentile and R. Ferretti

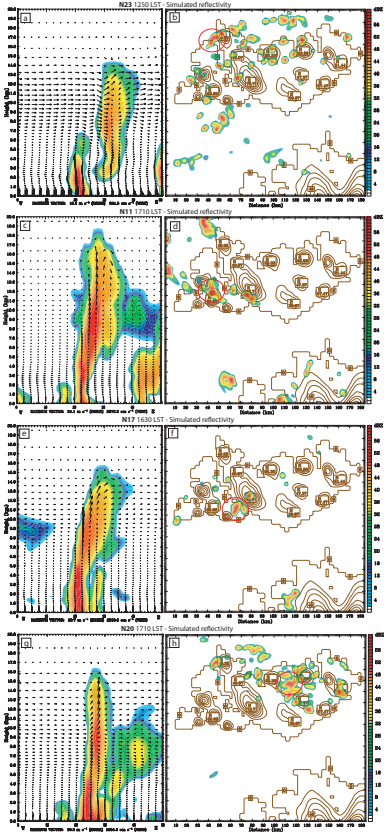

Figure 6. Sections at the maximum development of the Hector events N23, N11, N17 and N20. **(a)**, **(c)** and **(e)** Simulated vertical radar reflectivity (dBZ; filled color) and vertical wind, the section is taken along the red circle reported in the right panel. **(b)**, **(d)** and **(f)** Horizontal radar reflectivity (dBZ; filled color) and topography (brown).

NHESSD
3, 3621–3653, 2015

Seeking for key meteorological parameters to better understand Hector

S. Gentile and R. Ferretti

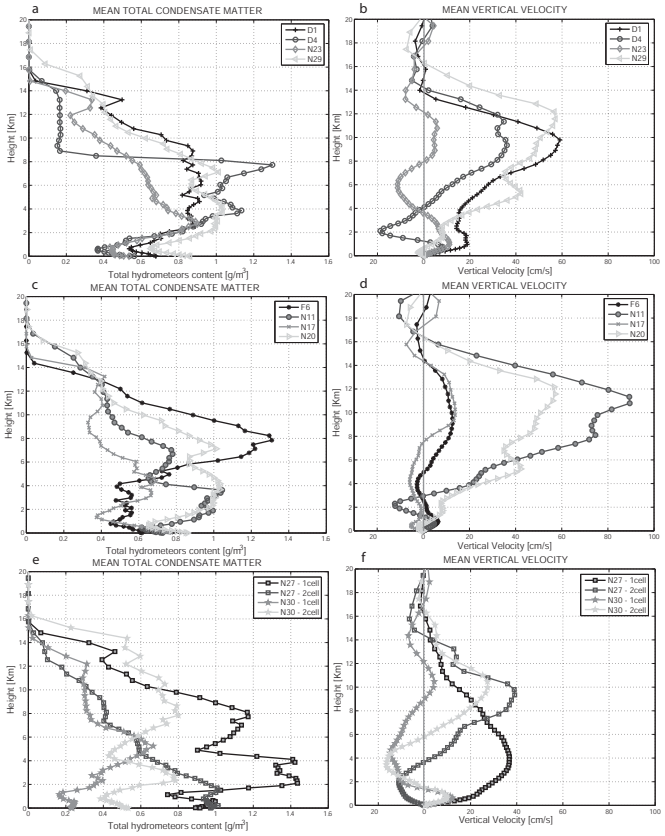

Figure 7. MM5 mean vertical profiles of cloud total condensate (sum of all hydrometeors) and vertical velocity at the maximum stage. Profiles are averaged for each layer within the volume encapsulating Hector.

NHESSD
3, 3621–3653, 2015

Seeking for key meteorological parameters to better understand Hector

S. Gentile and R. Ferretti

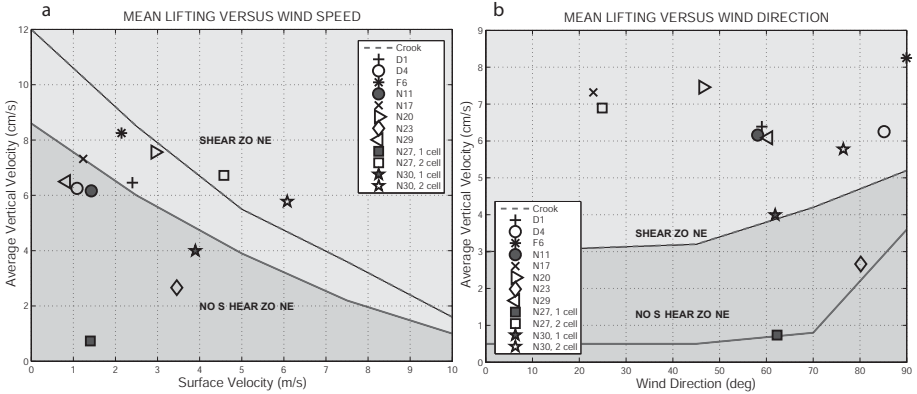

Figure 8. Crook's test: **(a)** and **(b)** show vertical velocity at 500 m extracted 3 h before the maximum development vs. surface wind speed **(a)** and surface wind direction **(b)**, both extracted at the start time. The figure reports two different regimes with a sheared (light gray, dashed line) and unsheared flow (dark gray, solid line) as studied by Crook.

NHESSD
3, 3621–3653, 2015

Seeking for key meteorological parameters to better understand Hector

S. Gentile and R. Ferretti

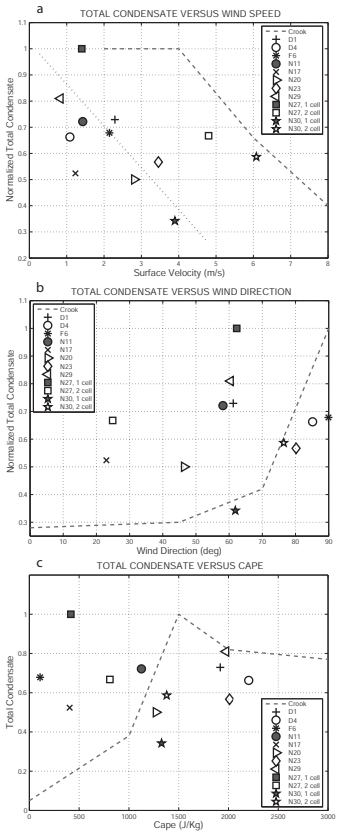

Figure 9. Crook's test: normalized total condensate extracted at the maximum stage and averaged into the Hector volume vs. surface wind speed **(a)**, surface wind direction **(b)** and CAPE **(c)**, extracted at the start time. The dashed gray line reports the Crook "ideal" trend, instead, the light gray dotted line in **(b)** the derived "real" trend.

NHESSD
3, 3621–3653, 2015